Journal of Optoelectronics and Advanced Materials Vol. 7, No. 3, June 2005, p. 1499 - 1509

STRUCTURAL CHARACTERIZATION AND OPTOELECTRONIC PROPERTIES OF BORON THERMALLY DIFFUSED SI (400)

E. Frantzeskakis, P. E. Tsakiridis, E. Hristoforou*

Laboratory of Physical Metallurgy, School of Mining and Metallurgical Engineering
National Technical University of Athens 9, Iroon Polytechniou Street, 157 80
Zografou, Athens, Greece

Thermal diffusion of boron into silicon single crystal at 1100 ^{o}C, followed by annealing, in inert atmosphere, has been investigated with respect to corresponding optoelectronic properties. A layer of boron powder, deposited on a silicon (400) wafer, was used as a dopant source for B. The cold resistance response of the films with respect to light of different wavelengths was used for the quantification of their optoelectronic properties. A correlation between the optoelectronic behavior and the structural characterization of the produced samples was also realized.

(Received April 27, 2005; accepted May 26, 2005)

Keywords: Silicon (400), Boron, Thermal Diffusion, Optoelectronic properties

1. Introduction

Silicon technology is more used than that of any other semiconductor and the diffusion of boron impurities is the first step of a plethora of device fabrication methods. Boron diffusion and the development of p-type semiconductors provide an essential stage before the construction of p-n junctions, which serve as the foundation of the physics of semiconductor devices and are of great importance both in modern electronic applications and in understanding other semiconductor devices. A p-n junction serves as a light source, as a light detector device (e.g. light emitting diodes) or even as a laser source [1,2]. A p-n junction comes into use for the construction of transistors, which are the basic parts of electronic circuits. Pure Si is an intrinsic semiconductor with an indirect bandgap of 1,12 eV at room temperature [3]. At the same temperature it is characterized by an intrinsic carrier concentration of 1.45×10^{16} /m^3 and intrinsic resistivity of 2,315 Ω.m [4].

Ion implantation is the one of the most common method of introducing dopant atoms for the fabrication of Si devices. However, there are limitations on this technique in the formation of shallow boron p-type junctions [5,6]. Boron requires low energy implantation of less than 5 keV, and at room temperature does not have sufficient energy to transform the silicon substrate to the amorphous state. Prior silicon ion implantation to transform the substrate surface to the amorphous state does not completely eliminate channeling tails. After ion implantation, it is necessary to use annealing temperatures greater than 900 °C to activate the dopant and to remove the ion implantation damage. The diffusivity of boron in silicon [7,8] and the transient-enhanced diffusion of the channeling tails during the thermal anneal make the control of shallow junctions using ion implantation difficult.

The above difficulties have led to the study of alternative doping techniques. Shallow p^+-n junctions have been fabricated by thermal diffusion of boron from spin-on dopants (SOD) [8,9]. Spin-on dopant deposited directly on a silicon substrate acts as a planar dopant source in thermal diffusion [10]. During thermal diffusion, boron can be evaporated from the SOD at the temperature of 1100 ^{o}C, across the separation gap to the product wafer.

* Corresponding author: eh@metal.ntua.gr

In this reaction, doped Si is formed on the surface of the product wafer and becomes a dopant source for elemental boron, which diffuses into the silicon substrate.

Boron (B) has been one of most important dopants in Si device fabrication for several decades, and its peculiar behavior in Si crystal or at Si surfaces has attracted much attention [11-13]. Particularly, it has been revealed that B atoms have a covalent radius smaller than that of the Si substrate atoms and therefore prefer to be incorporated into the subsurface of Si(111) or Si(100) [14,15]. However, the so far published literature has given little attention to the boron diffusion into the Si(400) subsurface.

The present research work presents the results of the boron thermal diffusion in inertial atmosphere (Ar) into Si (400) oriented wafer, which had been produced by the Czochralski method. After the thermal diffusion of boron impurities into its lattice, silicon becomes a p-type doped semiconductor. Silicon lattice becomes rich in negative ions of acceptors and positively charged holes, which serve as the main type of carriers at p-type semiconductors. For the creation of conductivity carriers the supply of energy should not exceed the value of the energy bandgap. It should be however, greater than the difference $E_A - E_V$, where E_A stands for the energy level of the acceptor impurities and E_V is the top of the silicon valence band. Consequently there is a systematic reduction of the observable bandgap in relation to the increase of impurities concentration.

We attempted to quantify the reduction of energy bandgap in relation to the experimental constants of boron diffusion. For the above purpose were used the Broadband Interference Filters (created by Edmund Industrial Optics), with a remarkably narrow bandwidth, in order to acquire high sensitivity and precision, as far as wavelength measurements are concerned. The cold resistance of the specimens was used for the quantification of their optoelectronic properties. Finally, their optoelectronic behavior was correlated with respect to the structure of the samples, which was determined using the technique of X-Ray Diffraction (XRD)

2. Experimental

The experimental (400) oriented silicon wafer was produced by the Czochralski method. The substrate was divided into pieces of 12×12 mm. Boron was spread in powder and it was subsequently diffused into the specimens using heat treatment in a furnace of inertial atmosphere. After the insertion of the sample into the furnace, vacuum was created in order to drive the atmospheric air away. The above process was repeated many times in order to achieve high standards of purity. Finally, a steady circulation of pure Argon was realized into the furnace, during thermal diffusion. The thermal diffusions attempts were accomplished at 1100 ^{o}C. The specimens remained at the above temperature for three different time limits (1, 2 and 4h). They were subsequently annealed using the same Ar-atmosphere furnace. The annealing temperature was at 1100 ^{o}C and the samples were treated for 1 and 2 hours, regardless of their diffusion time length. Slow cooling was also applied in order not to distruct the Si wafer structure. To the above temporal experimental constants, we had to add the time length needed to reach the desirable temperature, as well as the time length needed for the cooling of the furnace and the exertion of the samples.

The samples obtained as described above were mineralogically analyzed by X-ray diffraction (XRD), using a Siemens D5000 diffractometer with nickel-filtered CuKα1 radiation (=1.5405Å), 40 kV and 30 mA.

The cold resistivity of the samples was measured in relation the wavelength of the incident light. The above process was accomplished inside a black box. The light source was a conventional bulb of white light produced by OSRAM. The operation voltage was 12V and it could achieve current power of 50 W. The achievement of monochromatic radiation was made after the application of sensitive filters produced by Edmund Industrial Optics, with the commercial name of Broadband Intereference Filters. Nine (9) filters were totally used, with wavelengths ranging from 400 to 900 nm. The resistivity of the samples was measured using a 4-point resistance measurement device. Four spring probes with needle point (produced by RS-components) were placed in a linear geometry on the surface of the specimens. The distance between two successive spring probes was 3 mm. The external spring probes served for the circulation of the electric current, while the internal for the potential difference measurement. The constant distance between two successive spring

probes, as well as the width equality of the specimens, rendered their electric resistance R satisfactory means of comparison between different samples. Every sample remained under each of the 9 filters for 10 minutes. Subsequently, the arithmetic mean of the range of the above measurements was calculated and the above process was revised after a 10-minute intermission. The total number of revisions was 5 and the standard deviation of the measurements was determined at 4%. A Peltier temperature transducer and a sensitive thermocouple were used for maintaining the thin film temperature at 25 ^{o}C $\pm$1 ^{o}C.

3. Results and discussion

3.1 Structural characterization by X-ray diffraction

The XRD diagram of unprocessed single-crystalline silicon is presented in Fig. 1. With the term "unprocessed", we identify the sample, which was not subjected in any laboratory treatment (e.g. thermal diffusion or annealing).

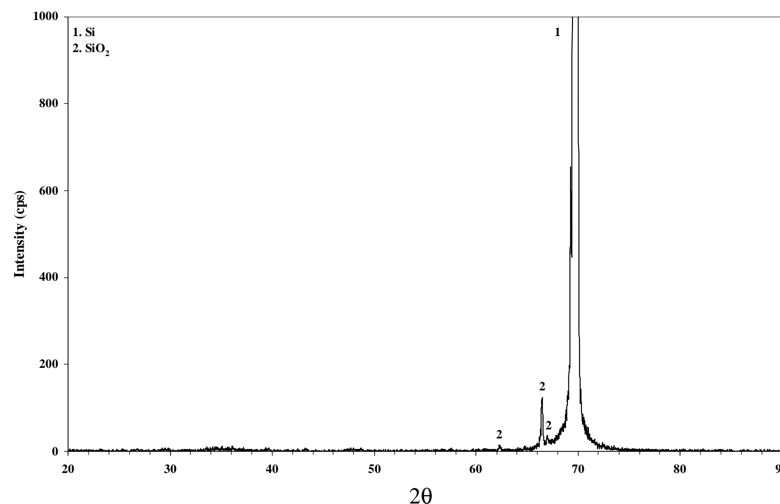

Fig. 1. (400) oriented silicon wafer produced by the Czochralski method.

The peak of single-crystalline silicon corresponds to the value 2θ = 69.74^{o} and the reflection plane is (400). The lower peaks on the left side of the prime one correspond to SiO_2. Silicon dioxide is a result of a slight oxidation of the specific sample due to the atmospheric air.

As it is shown in Fig. 2, after boron thermal diffusion for 1h, the treated sample has a response like an amorphous material. There is a complete absence of the characteristic peaks, which are the result of a crystalline symmetry. Instead of them, there is an "amorphous bell" in the area between 65° and 73°, as far as the Bragg angle is concerned. The crystalline symmetry of the material was destroyed after diffusion of boron impurities into its lattice. Boron atoms acquire both vacant lattice positions and interstitial positions, while they also drive many of the Si lattice atoms away of their former positions. The subsequent random changes of lattice distances justify the existence of the characteristic "amorphous bell". There is no characteristic lattice constant, which corresponds to a single Bragg angle. There is however a large number of different distances, which have as a result the slightly increased intensity of the diffracted radiation for a wide range of angles. Silicon lattice has been destroyed in a great extent and therefore the material is characterized as amorphous [16].

After the annealing process, the lattice symmetry is restored (Fig. 2). Silicon is again crystallized under the direction (400). Due to the annealing process, the boron impurities have acquired enough energy, to move and fill the existing vacant positions in the silicon lattice.

Subsequently, the latter is "reconstructed" and the characteristic peak of the (400) direction appears in its XRD diagram again. The atoms of boron, which diffuse into the silicon lattice, move from one vacant lattice position to another only by 2%. Boron diffusion in Si is dominated to a degree of more than 98% by a "Si-interstitial" mechanism. Boron substitutional atoms interact with interstitial silicon atoms of a tetrahedral symmetry, and they fall into interstitial positions of hexagonal symmetry. Afterwards, they interchange positions with a substitutional silicon atom, and thus they return into the silicon lattice [17].

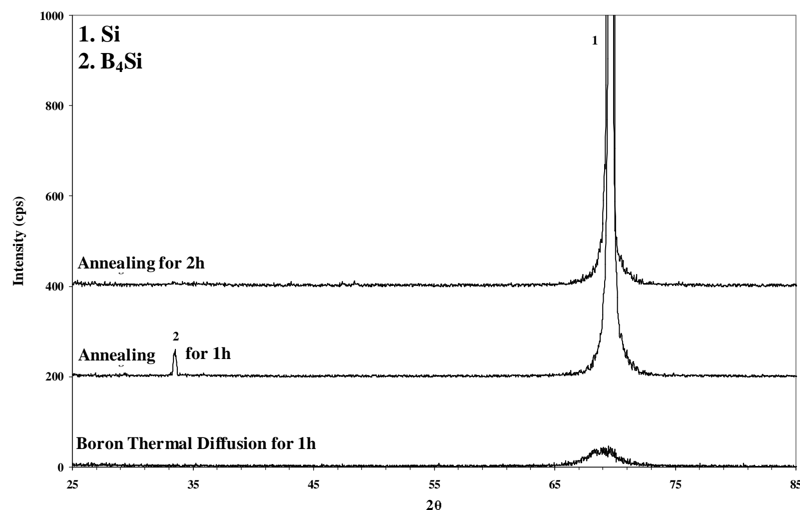

Fig. 2. Boron thermal diffusion for 1 hour. Annealing for 1 and 2 hours in inert atmosphere.

Filling of silicon vacant positions by boron impurities looks impossible. The two elements have completely different crystalline lattices (diamond lattice for Si, rhombohedral lattice for B). Moreover, there is a big difference between their atomic radius (1.46 and 0.87 Å correspondingly). Finally, there is also a significant difference as far as their electro-negativity ant their atomic valence are concerned. According to the Hume – Rothery criteria, only elements of the same crystal structure and similar values for their atomic radii, electro negativity and valence, can form solid solutions of substitution. None of the above criteria for a solid solution Si – B. However, it must be taken into account that the number of vacant interstitial positions is extremely small (it is $1/10^{13}$ in relation to the atoms of Si at room temperature). Subsequently, the solubility of B into Si is negligible to regard their interaction as a solid solution of substitution. This negligible solubility is nevertheless satisfactory for the formation of a p-type semiconductor. As a result, the filling of the vacant lattice position can be justified by the mechanism, which was described in the previous paragraph.

There is an additional characteristic peak in Fig. 2. It corresponds to the chemical compound B_4Si (silicon tetraborite), which was created after annealing for 1h and it is crystallized under the (021) direction. Silicon tetraborite disappears after 1 additional hour of annealing. This is because the B atoms gain enough energy to diffuse into the silicon lattice completely. Therefore they do not form any additional chemical compound.

The lack of crystal symmetry is also observed for the specimen, which has undergone the boron diffusion process for 2h at the temperature of 1100 °C (Fig. 3). The violent diffusion of boron impurities, in both substitutional and interstitial positions, has again destroyed the crystal symmetry of the material. As a result, the diffracted radiation has a slightly increased intensity for a wide range of angles (~65°-74°), instead of the characteristic peak of the (400) oriented silicon wafer. After the annealing process for 1 or 2h, the symmetry is restored (Fig. 3). The same phenomenon, which was described in the previous paragraph, can be observed: the existence of an additional characteristic peak, which corresponds to the (021) oriented B_4Si. Furthermore, the atoms of silicon have acquired enough energy to diffuse into the silicon lattice and they do not form any other chemical compound. Therefore, the absence of the B_4Si peak is justified.

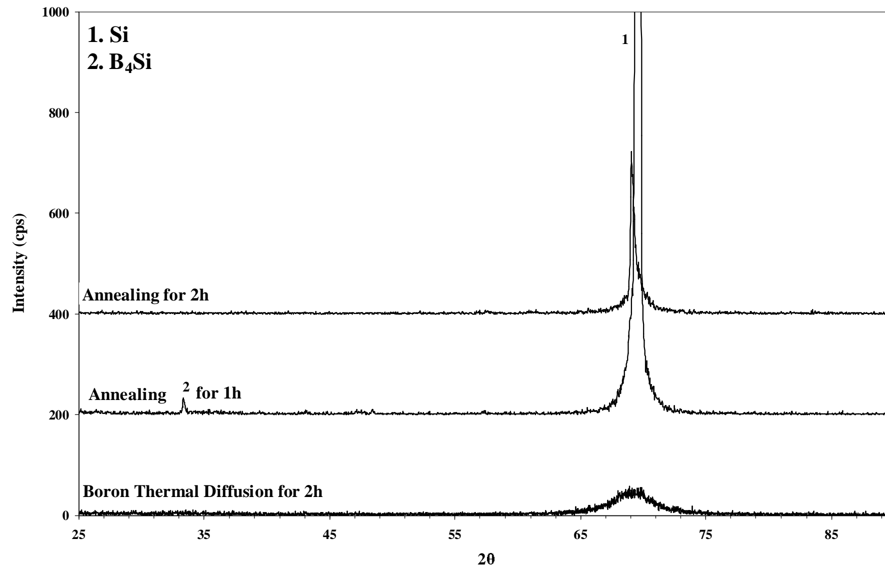

Fig. 3. Boron thermal diffusion for 2 hour. Annealing for 1 and 2 hours in inert atmosphere.

After a thermal diffusion for 4h at the temperature of 1100 °C, the amorphous character of the material is again obvious (Fig. 4). However, the lack of crystal symmetry remains after annealing for 1h. The impurity atoms have destroyed the crystal lattice in such a big extent after the 4h diffusion process, that the acquired energy is not enough to drive them into lattice positions and restore the former symmetry. More energy is needed, and it is acquired after annealing for 2h at the same temperature. The material is again crystallized under the (400) direction and the boron atoms have been diffused into the vacant positions according to the "Si-interstitial" mechanism, which was described above.

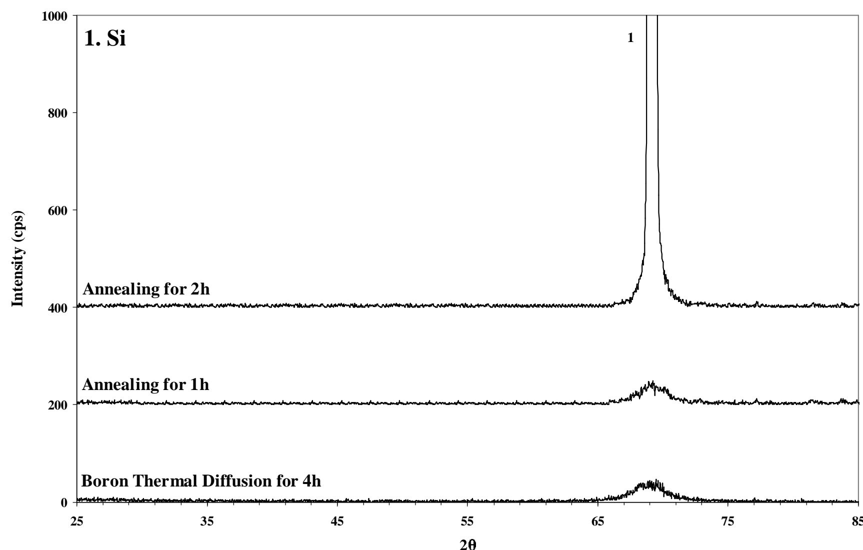

Fig. 4. Boron thermal diffusion for 4 hour. Annealing for 1 and 2 hours in inert atmosphere.

In Fig. 5, the characteristic peaks of the samples are given, which have undergone the processes of annealing for 1 and 2h, after thermal diffusion for 1h. They are presented in relation to the peak of untreated (400) single-crystalline silicon. There is a systematic shift of the characteristic peak towards the left side of the diagram when the annealing time length increases. The values of the Bragg angles for the three samples are 69.74^o, 69.64^o and 69.56^o, correspondingly. The diffusion of boron impurities into the silicon lattice changes the atomic distances. Boron atoms acquire lattice positions by filling former vacancies. Therefore, lattice contraction around these vacancies is no longer possible, resulting in an increase in the average distance of the Si planes. According to the Bragg law, an increase in "d" will result in a decrease in sinθ. This is exactly the reason why there is a shift in the XRD diagrams towards smaller values of θ. After annealing for 1 h, the compound B_4Si was also constructed and as a result, fewer atoms of B diffused into the lattice positions, than after annealing for 2h. The atomic distances have been altered in a lower degree and thus, the corresponding peak is at a higher value of Bragg angles.

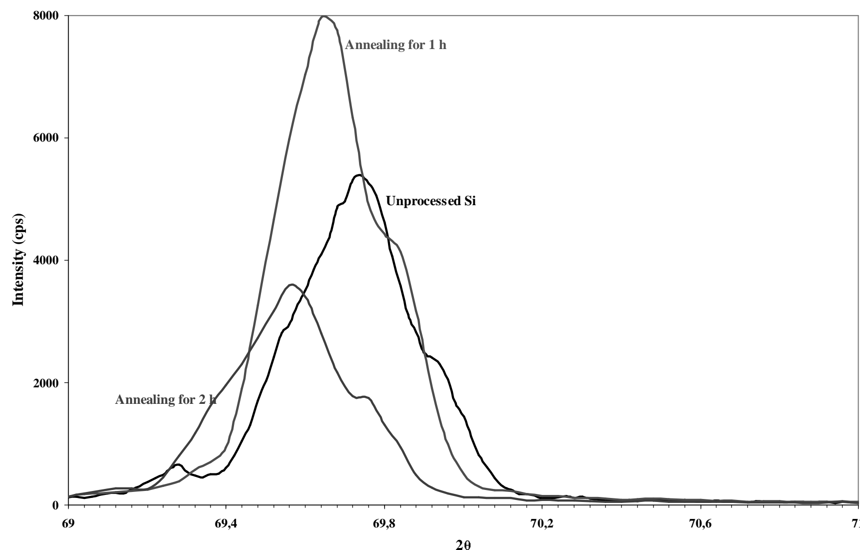

Fig. 5. Comparative diagram of the (400) oriented Si characteristic peak for boron thermal diffusion for 1 hour.

The same phenomenon, even in a greater degree, can be observed after a comparison of the characteristic peaks of the samples which have undergone the process of annealing for 1 and 2h, after thermal diffusion for 2h. As presented in Fig. 6, the characteristic peak of the specimens shifts towards even lower values of Bragg angles, in relation to the samples of boron thermal diffusion for 1h. The values of Bragg angles for the samples are 69,52^o and 69,04^o after 1 and 2h of annealing correspondingly. The diffusion of boron impurities is now greater because the time length of the process has been doubled. The same phenomenon can be observed for the sample, which has been treated with boron for 4h and has been afterwards annealed for 2h (Fig. 7). The systematic left-shift of the characteristic peak of the (400) Si is a direct consequence of the diffusion of boron impurities into lattice positions.

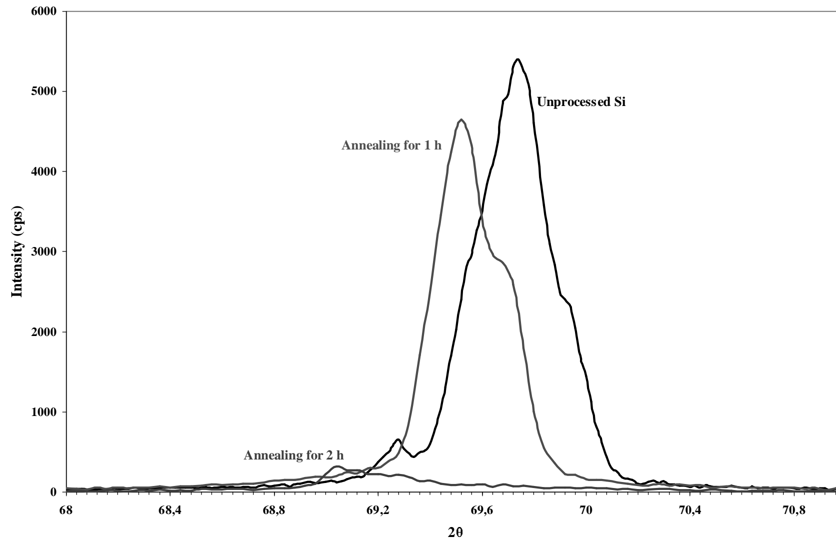

Fig. 6. Comparative diagram of the (400) oriented Si characteristic peak for boron thermal diffusion for 2 hour.

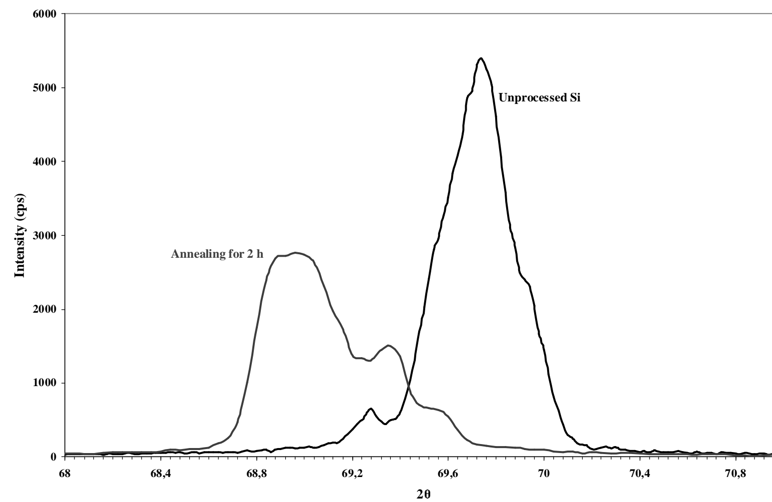

Fig. 7. Comparative diagram of the (400) oriented Si characteristic peak for boron thermal diffusion for 4 hour.

3.2 Electrical properties

The results of the electrical resistance, in relation to the wavelength of the incident light (R(λ) diagram), of the untreated (400) silicon are shown in Fig. 8. There is an abrupt increase of the semiconductor resistance in the vicinity of 450-500 nm. In the above wavelength area, there is a stimulation of the intrinsic carrier generation of Si. The energy which corresponds to 450 nm is high enough to move electrons from the valence to the conduction band of the material. However, energy of 500 nm is not sufficient for surpassing the energy bandgap. After the shift of electrons into the valence band because of the incident radiation, the semiconductor's carrier density increases. There are now holes in the valence band, as well as free electrons in the conduction band. Both types of carriers contribute to the increase of silicon conductivity, for wavelengths shorter than 450 nm.

Therefore, there is a steep decrease in the electric resistance for higher values of energy (or lower values of wavelength). As far as long wavelengths are concerned, room temperature is the prime reason for the generation of electric carriers. However, at lower values of λ, incident monochromatic radiation is, as described above, instrumental.

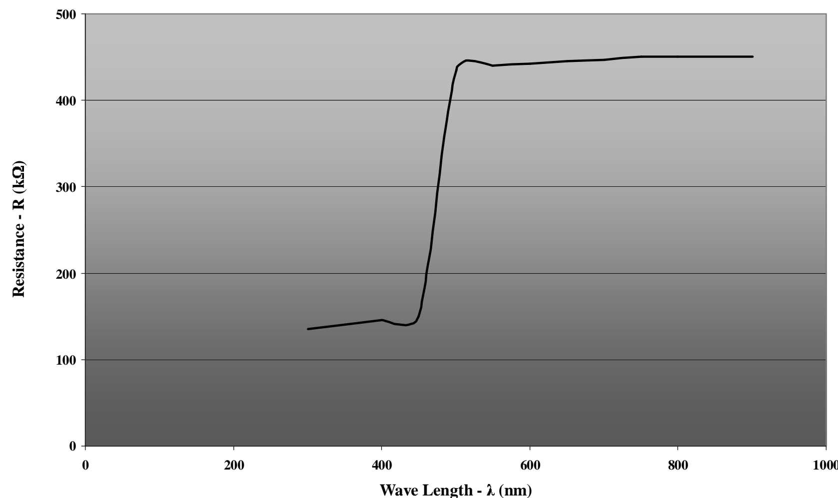

Fig. 8. Electrical resistivity in relation to the wavelength of the incident light for: (400) oriented silicon wafer.

After the diffusion of boron impurities for 1h, a p-type semiconductor has been created. The external mechanism of generation of electric carriers plays a fundamental role. It is possible that after a small supply of energy, some electrons move from the valence band to the energy level of the acceptor impurities. The holes of the valence band, which are left behind them, serve as the majority carriers, while the electrons of the conduction band as the minority carriers.

The results of resistivity in relation with wavelength of the incident light, after undergoing boron thermal diffusion for 1h and after annealing for 1h and 2h are given in Fig. 9. Concerning the sample after thermal diffusion, which presents an amorphous structure, boron atoms have diffused into interstitial positions. The holes created by them can move very easily, because they do not interfere with the silicon lattice. This can be done with a small supply of energy, acquired even by normal room temperature. Thus, the sample's resistivity is much lower than pure silicon, even when the incident light does not have a fundamental role (high wavelengths). There is a shift of the energy gap towards higher values of wavelength. Subsequently, there is a decrease in its energy value. The external mechanism for the stimulation of acceptor's impurities can be started in much lower values of the incident's radiation frequency. A combination of the external and the internal mechanism for the generation of carriers makes the surpassing of the energy gap feasible for lower values of energy. The abrupt increase in the conductivity of the sample happens now in the vicinity of 600 nm. For high values of energy, the internal mechanism of carrier's generation prevails over the external. Therefore, the carriers' density has no big difference than pure silicon, and the two specimens have similar conductivity values at short wavelengths.

After annealing for 1h, a significant difference remains between the resistance values at high wavelengths. There is still an important number of interstitial boron atoms, which can provide electrical carriers due to energy acquired at room temperature. The above difference does not longer exist after annealing for 2h. Most of boron atoms have now diffused into lattice positions. There is also a right-shift of the energy gap value in comparison with pure silicon. The external mechanism for generation of conductivity carriers, results into the abrupt change of the electric resistance at lower energy values. The energy gap that needs to be surpassed by electrons is now smaller (about 500 nm in terms of λ) than the unprocessed Si sample. However at low wavelengths, the internal mechanism for generation of carriers prevails, and the three samples have similar conductivity values.

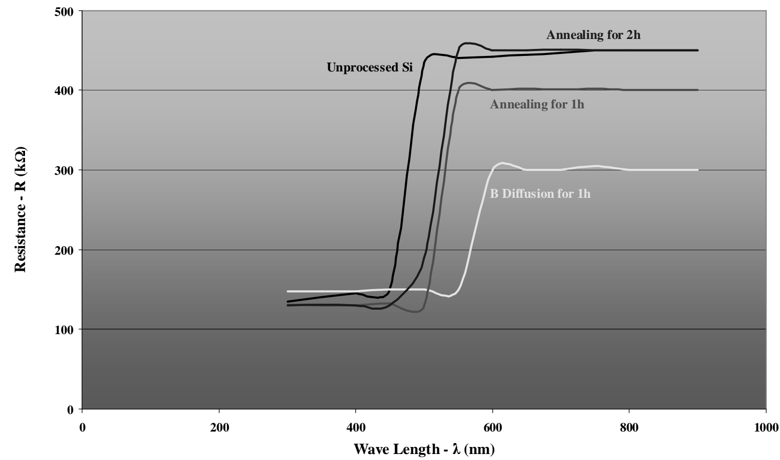

Fig. 9. Thermal diffusion for 1 h and annealing for 1h and 2h. Electrical Resistivity in relation to the wavelength of the incident light

The conclusions of the previous paragraphs extend to the case of the samples that have been treated with boron for 2 hours. The results of resistivity in relation with wavelength of the incident light, after undergoing boron thermal diffusion for 2h and after annealing for 1 and 2 hours are given in Fig. 10. They are presented in contrast to pure silicon.

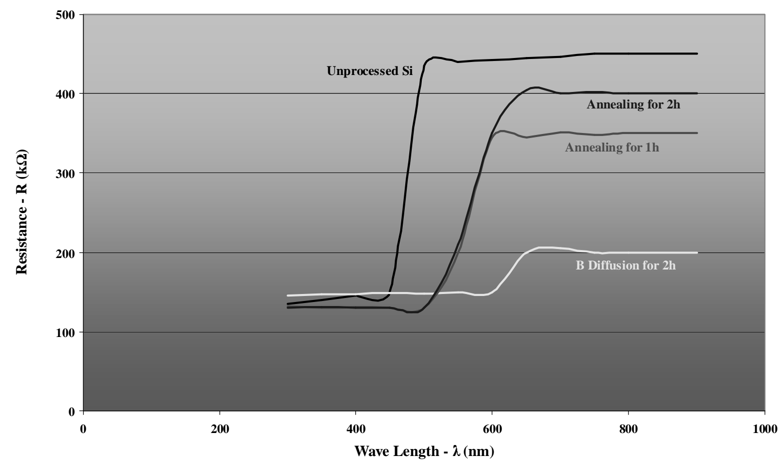

Fig. 10. Thermal diffusion for 2 h and annealing for 1h and 2h. Electrical Resistivity in relation to the wavelength of the incident light.

The sample has an amorphous structure because of the violent diffusion of boron impurities, the occupation of interstitial positions and the destruction of the silicon lattice. The interstitial impurity atoms can become the source of generation and propagation of holes after a small supply of energy. The supply of energy can be due to normal room temperature. At high wavelengths radiation has no significant role, and therefore the two specimens have huge differences as far as their electrical conductivity is concerned. This phenomenon is even greater than it was after 1h of annealing because now there are more interstitial impurity atoms.

The abrupt change in the sample’s conductivity happens even at lower energy values in contrast to the previous sample. The presence of more impurity atoms makes the influence of the external mechanism for the generation of carriers even greater. At lower wavelength values the internal mechanism prevails, and the observable differences in the specimens’ resistivity are small.

The change of the sample's conductivity is smaller than the specimen which was treated with boron for 1h. There are now more impurities in interstitial positions and therefore the thermal generation of electrical carriers is greater. This fact renders the influence of radiation into the generation of carriers trivial.

After annealing for 1h and 2h, at high wavelengths the difference in the conductivity of the samples is due to the presence of boron atoms in interstitial positions. The difference becomes less when the time length of annealing increases. The samples which contain boron have a lower energy gap value (about 600 nm in terms of λ) than pure silicon. The external mechanism for the generation of electrical carriers, results into the increase of conductivity at lower energy values of incident radiation. However, at high values of energy the three samples have similar values of resistivity.

Fig. 11 shows the resistivity results vs the wavelength of the incident radiation for the samples, which have been treated with boron for 4h and annealed for 1h and 2h. The conclusions drawn from Figs. 9 and 10 are still valid and magnified. If we consider the unprocessed Si sample and the sample which has undergone thermal diffusion for 4h without annealing, we can observe that the difference between the electrical resistances of the two specimens is quite large at low and negligible at high energy values. The abrupt change of the electrical conductivity of the second sample is very small. The influence of the incident radiation is obvious in the vicinity of 650 nm.

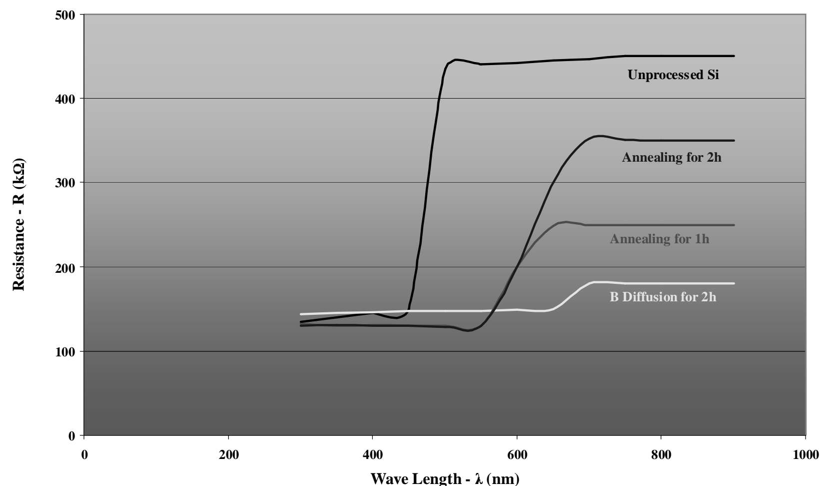

Fig. 11. Thermal diffusion for 4 h and annealing for 1h and 2h. Electrical resistivity in relation to the wavelength of the incident light

After annealing for 1 and 2h, at high wavelengths, the difference in the value of the electrical resistance, in contrast to pure silicon, decreases in proportion to the time length of the annealing process. At low wavelengths, the internal mechanism for the generation of carriers prevails, and there is no observable difference in the conductivity. Finally, there is a further decrease in the value of the energy gap, which needs to be surpassed in order to generate carriers. The value of the energy gap, in terms of λ, is now in the vicinity of 650 nm.

All the above described samples, which contain boron impurities, are p-type doped semiconductors and they have much smaller energy gap values than pure silicon. P-type semiconductors have a relatively high density of conductivity carriers for small amounts of supplied energy. Thus, the abrupt change in their resistance happens at much higher wavelength values.

4. Conclusions

Boron thermally diffused Si (400) wafers were optoelectronically characterized and structurally studied. The optoelectronic properties have been related to the structure of the film after thermal diffusion and creation of the p-type semiconductor.

References

[1] S. Simeonov, E. Kafediijska, A. Szekeres, C. Ristoscu, E. Gyorgy, I. N. Mihailescu, G. N. Mikhailova, J. Optoelectron. Adv. Mater. **2**(1), 99 (2000).
[2] M. Lipinski, P. Panek, R. Ciach, J. Optoelectron. Adv. Mater. **5**(5), 1365 (2003).
[3] Cojocaru, V. Karavanskii, V. Pasat, V. Chumash, J. Optoelectron. Adv. Mater. **1**(2), 67 (1999).
[4] G. S. Adriaenssens, H. Z. Song, V. I. Arkhipov, E. V. Emelianova, W. M. M. Kessels, A. H. M. Smets, B. A. Korevaar, M. C. M. van de Sanden, J. Optoelectron. Adv. Mater. **2**(1), 31 (2000).
[5] W. Eichhammer, M. Hageali, R. Stuck, P. Siffert, Applied Physics A-Materials Science and Processing **50** (4), 405 (1990).
[6] S. N. Hong, G. A. Ruggles, J. J. Wortman, M. C. Ozturk, IEEE Transactions on Electron Devices **38**(3), 476 (1991).
[7] R. B. Fair, Proceedings of the IEEE, **78**(11), 1687 (1990).
[8] M. Nolan, T. Perova, R. A. Moore, H. S. Gamble, Journal of Non-Crystalline Solids **254**(1-3), 89 (1999).
[9] T. A. Briantseva, Z. M. Lebedeva, D. V. Lioubtchenko, I. A. Markov, M. Nolan, T. S. Perova, R. A. Moore, Applied Surface Science **156**(1-4), 21 (2000).
[10] E. Ling, P. Maguire, H. S. Gamble, B. M. Armstrong, Low resistivity, 100-NM PN Junctions for submicron CMOS, Journal of the Electrochemical Society **134**(3), C118 (1987).
[11] G. Glass, H. Kim, P. Desjardins, N. Taylor, T. Spila, Q. Lu, J.E. Greene, Physical Review B, **61**(11), 7628 (2000).
[12] Z. Zhang, K. Sumitomo, Surface Science **576**(1-3), 83 (2005).
[13] M. Bulinski, V. Kuncser, D. Cristea, C. Plapcianu, S. Krautwald, H. Franke, F. E. Wagner, G. Filoti, J. Optoelectron. Adv. Mater. **5**(1), 331 (2003).
[14] M. A. Kulakov, Z. Zhang, A. V. Zotov, B. Bullemer, I. Eisele, Applied Surface Science **103**(4), 443 (1996).
[15] Y. J. Wang, R. J. Hamers, E. Kaxiras, Physical Review Letters **74**(3), 403 (1995).
[16] M. Popescu, H. Bradaczek, J. Optoelectron. Adv. Mater. **1**(1), 5 (1999).
[17] W. Windl, M. M. Bunea, R. Stumpf, S. T. Dunham, M. P. Masquelier, Physical Review Letters, **84**(21), 4345 (1999).